

# XUV Fluorescence Detection of Laser-Cooled Stored Relativistic Ions

Ken Ueberholz <sup>1,\*</sup>, Lars Bozyk <sup>2</sup>, Michael Bussmann <sup>3,4</sup>, Noah Eizenhöfer <sup>5</sup>, Volker Hannen <sup>1</sup>, Max Horst <sup>6,7</sup>, Daniel Kiefer <sup>5</sup>, Nils Kiefer <sup>8</sup>, Sebastian Klammes <sup>2</sup>, Thomas Kühl <sup>2,9</sup>, Benedikt Langfeld <sup>5,7</sup>, Markus Loeser <sup>4</sup>, Xinwen Ma <sup>10</sup>, Wilfried Nörtershäuser <sup>6,7</sup>, Rodolfo Sánchez <sup>2</sup>, Ulrich Schramm <sup>4,11</sup>, Mathias Siebold <sup>4</sup>, Peter Spiller <sup>2</sup>, Markus Steck <sup>2</sup>, Thomas Stöhlker <sup>2,9,12</sup>, Thomas Walther <sup>5,7</sup>, Hanbing Wang <sup>10</sup>, Christian Weinheimer <sup>1</sup>, Weiqiang Wen <sup>10</sup> and Danyal Winters <sup>2</sup>

<sup>1</sup> Institute of Nuclear Physics, University of Münster, 48149 Münster, Germany

<sup>2</sup> GSI Helmholtzzentrum für Schwerionenforschung GmbH, 64291 Darmstadt, Germany

<sup>3</sup> CASUS Görlitz, 02826 Görlitz, Germany

<sup>4</sup> HZDR Dresden, Institut für Radiation Physics, 01328 Dresden, Germany

<sup>5</sup> Institute of Applied Physics, TU Darmstadt, 64289 Darmstadt, Germany

<sup>6</sup> Institute of Nuclear Physics, TU Darmstadt, 64289 Darmstadt, Germany

<sup>7</sup> HFHF Darmstadt, Department for Atomic and Plasma Physics, 64289 Darmstadt, Germany

<sup>8</sup> Institut für Dünne Schichten und Synchrotronstrahlung, University Kassel, 34127 Kassel, Germany

<sup>9</sup> HI Jena, Department of Photon and Particle Spectroscopy, 07743 Jena, Germany

<sup>10</sup> IMP Lanzhou, Institute of Modern Physics, Lanzhou 730000, China

<sup>11</sup> TU Dresden, Institute of Nuclear and Particle Physics, 01069 Dresden, Germany

<sup>12</sup> Institut für Optik und Quantenelektronik, Friedrich-Schiller-Universität Jena, 07743 Jena, Germany

\* Correspondence: k\_uebe01@wwu.de

† Current address: Institut für Kernphysik, Westfälische Wilhelms-Universität Münster, Wilhelm-Klemm-Str. 9, 48149 Münster, Germany.



**Citation:** Ueberholz, K.; Bozyk, L.; Bussmann, M.; Eizenhöfer, N.; Hannen, V.; Horst, M.; Kiefer, D.; Kiefer, N.; Klammes, S.; Kühl, T.; et al. XUV Fluorescence Detection of Laser-Cooled Stored Relativistic Ions. *Atoms* **2023**, *11*, 39. <https://doi.org/10.3390/atoms11020039>

Academic Editors: Izumi Murakami, Daiji Kato, Hiroyuki A. Sakaue and Hajime Tanuma

Received: 31 October 2022

Revised: 18 January 2023

Accepted: 2 February 2023

Published: 13 February 2023



**Copyright:** © 2023 by the authors. Licensee MDPI, Basel, Switzerland. This article is an open access article distributed under the terms and conditions of the Creative Commons Attribution (CC BY) license (<https://creativecommons.org/licenses/by/4.0/>).

**Abstract:** An improved moveable in vacuo XUV fluorescence detection system was employed for the laser cooling of bunched relativistic ( $\beta = 0.47$ ) carbon ions at the Experimental Storage Ring (ESR) of GSI Helmholtzzentrum Darmstadt, Germany. Strongly Doppler boosted XUV fluorescence ( $\sim 90$  nm) was emitted from the ions in a forward light cone after laser excitation of the  $2s-2p$  transition ( $\sim 155$  nm) by a new tunable pulsed UV laser system (257 nm). It was shown that the detected fluorescence strongly depends on the position of the detector around the bunched ion beam and on the delay ( $\sim$  ns) between the ion bunches and the laser pulses. In addition, the fluorescence information could be directly combined with the revolution frequencies of the ions (and their longitudinal momentum spread), which were recorded using the Schottky resonator at the ESR. These fluorescence detection features are required for future laser cooling experiments at highly relativistic energies (up to  $\gamma \sim 13$ ) and high intensities (up to  $10^{11}$  particles) of ion beams in the new heavy ion synchrotron SIS100 at FAIR.

**Keywords:** fluorescence; laser cooling; pulsed lasers; Schottky spectra; ESR; SIS100

## 1. Introduction

High-precision experiments on ions stored at relativistic velocities demand a narrow longitudinal momentum distribution of the ion beam, which can only be achieved using cooling techniques. At the Experimental Storage Ring (ESR) at GSI, electron cooling is being used [1] to cool beams of highly charged ions and achieve low relative momentum spreads of  $\Delta p/p \approx 10^{-5}$  [2]. However, the efficiency of this method is limited for ion beams of higher energy, as expected at the currently constructed heavy ion synchrotron SIS100 at FAIR. Stochastic cooling is limited to low particle intensities, making laser cooling the most promising cooling method for the SIS100 [3]. Laser cooling uses a suitable (fast and closed) electronic transition in an ion that is excited by laser photons from co-

and counterpropagating laser beams, transferring energy and momentum to the ions. The ions subsequently de-excite through the isotropic emission of fluorescence photons (accompanied by a recoil of the ion) [4]. The net result is a deceleration of ions which are slightly too fast, being excited by the counterpropagating laser light, and an acceleration of slower ions in resonance with the copropagating laser. For relativistic ion beams, where a large Doppler shift of the laser wavelength is observed in the rest frame of the ions, only excitation by a counterpropagating laser beam is technically feasible.

In order to only decelerate the ions that are too fast, a counteracting force is also required to achieve true cooling. This RF bucket force is provided by a harmonic bunching of the ion beam at a frequency ( $f_b$ ) which is an integer multiple ( $h$ ) of the ion revolution frequency ( $f_{rev}$ ) in the ESR, i.e.,  $f_b = h \cdot f_{rev}$  ( $\sim 9$  MHz). When a pulsed laser system is used, a wide range of ion velocities can be addressed simultaneously, leading to a higher laser cooling efficiency [5] if a good spatial and temporal overlap between the laser beam and the ion beam is ensured. Observation of the fluorescence is the best and most direct method to verify and optimize the overlap in energy space and time of the laser pulses and ion bunches. Therefore, a specialized detection system is needed to monitor the fluorescence. This paper reports first results (analysis ongoing) obtained with a redeployed and improved in vacuo XUV detection system [6] during a beamtime at the ESR in 2021. A more in-depth discussion of the experiment can be found in [7].

## 2. Experimental Setup and Parameters

The experiment was carried out at the Experimental Storage Ring (ESR) at GSI Helmholtzzentrum für Schwerionenforschung in Darmstadt, Germany. The ESR (see Figure 1, left) was built to store and cool beams of heavy ions at relativistic speeds [1] between 10 % and 90 % of  $c$  and with atomic numbers between 1 (proton) and 92 (uranium). It utilizes a total of six dipole magnets with a magnetic rigidity of up to 10 Tm and has a circumference of about 108 m. The ESR features an electron cooler suitable for voltages between 2 and 240 kV and a system for stochastic cooling (400 MeV/u). Being designed for experiments, the ESR can house multiple detection systems for various experiments in a 16.5 m long straight section of the ring.

The ion beam was spatially overlapped with a counterpropagating laser beam on the same straight section where the XUV fluorescence detector is located. The revolution frequency of the ions was measured with a Schottky resonator at the 189th harmonic ( $\sim 244$  MHz), while the emitted fluorescence photons were measured using the improved moveable in vacuo XUV detection system [8,9]. The principle of the XUV detector (shown in Figure 1 on the right) relies on the photoelectric effect and was successfully deployed in 2016 for laser spectroscopy of the  ${}^2S_{1/2} \rightarrow {}^2P_{1/2}, {}^2P_{3/2}$  transitions in stored and cooled relativistic  $C^{3+}$  ions [8]. The XUV detector's geometry is designed to collect forward emitted photons, taking into account the relativistic boost which causes the fluorescence photons to be emitted in a  $1/\gamma$  cone in the forward direction [10]. When fluorescence photons hit the (moveable) cathode, electrons are emitted and accelerated away from the cathode by an applied negative voltage. These electrons are then guided by an external (ex vacuo) magnetic field onto a microchannel plate (MCP) detector. This detection system was improved before the beamtime by installing a stepper motor-controlled linear drive for the motion of the cathode and by mounting an improved shielding to reduce the amount of stray laser light and unwanted charged particles arriving at the MCP. The stepper motor enables the operation of the detector with the cathode at intermediate positions between the parking position (where both signal and background rates are low) and the center of the beamline (where the opposite is the case). This therefore allows the optimization of the signal to background ratio. The new shielding reduces the background from the laser light and from charged particles created in the vicinity of the detector, e.g., by residual gas ionization or by an ion-getter pump located below the detection system. With the improved shielding, it was for the first time possible to run the detector and the ion-getter pump in parallel. While the beam-related background is still a problem, these changes were

important steps toward a more sensitive detection system. The tunable pulsed laser system was a frequency quadrupled distributed feedback (DFB) laser with a final wavelength of 257 nm. Repetition rates between 1 and 10 MHz and pulse lengths between 166 and 735 ps could be achieved with an average effective UV power of 200 mW at 735 ps pulse length in the ESR. A wavelength of 257 nm corresponds to the Doppler corrected energy needed to excite the  $^2S_{1/2} \rightarrow ^2P_{1/2}$  transition of the stored  $^{12}C^{3+}$  ions, which orbit the ESR at a velocity of 0.47 c, or equivalently, 122 MeV/u [7].

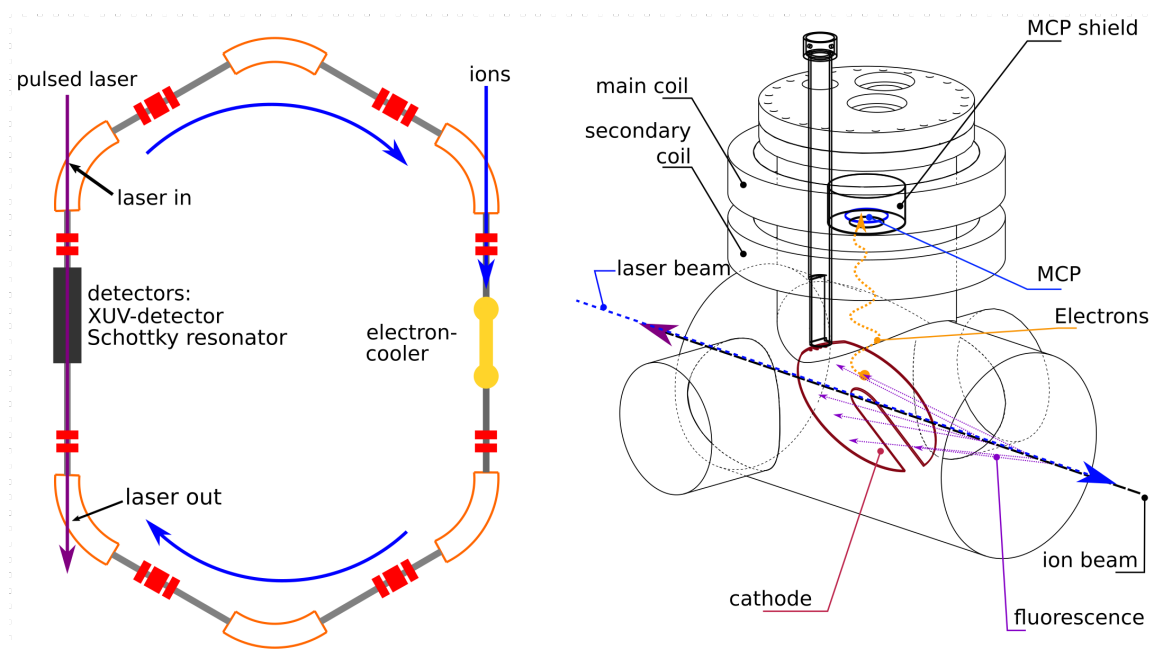


**Figure 1.** The Experimental Storage Ring (ESR) at GSI with the setup used for laser cooling experiments is shown on the left, and a schematic diagram of the XUV detector and its working principle is shown on the right [6].

### 3. First Results from the XUV Detector

One of the goals of the experiment was to investigate the rate of fluorescence photons resulting from the interaction between the laser pulses and the stored  $^{12}C^{3+}$  ions for a range of different experimental parameters, such as the timing between bunches and laser pulses. Firstly, the wavelength of the laser light was varied to match the Doppler shifted transition wavelength in the ion. Subsequently, the laser pulses were synchronized with the ion bunches, and an additional time delay was introduced to the laser pulses to shift the spatial overlap region of the laser pulses and the ion bunches over the entire straight section of the ESR. In the following sections, we will show the first results from these measurements, which clearly indicate the performance and possibilities offered by the XUV fluorescence detector.

#### 3.1. Laser Wavelength Scans

In order to set up the experiment, the electron cooler was turned on to decrease the longitudinal momentum spread of the ion beam. The laser wavelength was periodically varied from 257.238 nm to 257.235 nm in the form of a sawtooth function over a period of 20 s, as depicted in Figure 2. Here, all the data are plotted versus time, starting 5 s after the ion injection into the ESR. In panel 1, at the top, the XUV detector signal (fluorescence rate) is shown. In panel 2, in the middle, the laser wavelength is plotted, and in panel 3, at the bottom, the corresponding Schottky spectrum is shown. The recorded rate of the XUV detector was corrected for the background induced by stray laser photons and normalized to the ion beam (in order to correct for ion beam losses due to interactions with the residual

gas in the beam pipe) and shows distinct peaks. The laser light is firstly red-detuned and becomes more and more resonant with the Doppler shifted transition wavelength of the ions during the scan, leading to an increase in fluorescence rate. In the Schottky spectrum, the effect of the laser is observable as a clear drop of intensity (blue) at a particular frequency. This drop is caused by the fact that the laser light pushes these ions to slightly lower velocities (i.e., towards the intense central trace in the Schottky spectrum), which can be seen as an increase in intensity (green/yellow) at that point. When the laser wavelength is scanned, a corresponding trace can clearly be seen. In Figure 2, three laser scans are shown. The signal-to-noise ratio of the peaks increases with each of the three scans because the combined effect of the laser scans and the electron cooler push the ions to the central velocity more quickly than they are lost due to charge exchange with the residual gas.

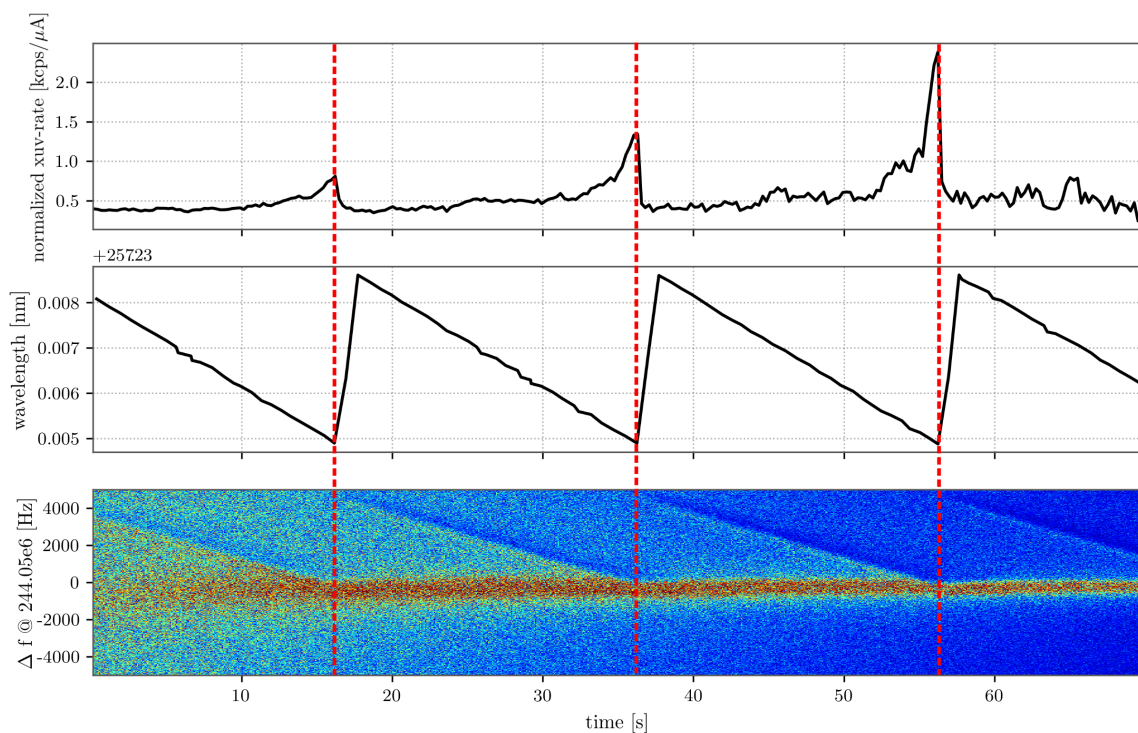


**Figure 2.** Laser scans of an electron-cooled coasting ion beam of  $^{12}\text{C}^{3+}$  ions at the ESR, plotted as a function of time. **Top:** the rate of the fluorescence photons detected by the XUV detector, **middle:** the laser wavelength, **bottom:** the Schottky spectrum.

The Schottky spectrum before the first laser scan can be seen on the far left of Figure 2, bottom panel, and the one after the last laser scan on the far right. The trace of the ion beam becomes smaller over time, but this is mainly due to continuous electron cooling and loss of ion beam intensity. Since the ion beam is not bunched, there is no laser cooling.

### 3.2. Laser Pulse Delay

Due to the geometry of the XUV detector (see Figure 1, right), only photons emitted in front of the detector can directly hit the cathode and produce electrons which are guided through electromagnetic fields to the MCP detector [6,8]. For fluorescence detection, it is important to position the spatial overlap region of the laser pulses and the ion bunches within the detection zone. To vary and thus optimize the position of this overlap region, the laser wavelength was fixed at 257.235 nm (resonance condition), and laser pulses were delayed in small (ns) steps with respect to the ion bunches to spatially move the overlap region along the straight section of the ESR. For these measurements, the ion beam was bunched at  $h = 7$ , i.e., at a bunching frequency of 7 times the ion revolution frequency (1.29 MHz), which is  $\sim 9$  MHz. The control voltage of the bunching amplitude was low, i.e.,

below 250 mV. To synchronize the laser pulses with the ion bunches, the repetition rate of the pulsed laser system was equally set to the bunching frequency ( $\sim 9$  MHz). Since the laser pulse generation could be set by a trigger, the laser pulses could also be delayed. A repetition rate of  $\sim 9$  MHz implies a time difference between successive pulses and bunches of about 110 ns. At a velocity of  $0.47c$ , it also takes about 110 ns for an ion bunch to cross the straight section of the ESR. These numbers imply that there must be a maximum in the fluorescence rate within a 110 ns range, and that this maximum occurs again 110 ns later. This has indeed been observed. The maximum was also quite narrow; delays of only a few ns caused clear changes in the fluorescence yield, as can be seen in Figure 3. This reflects the short detection zone and the short ion bunches (and laser pulses). Again, the data were corrected for the laser background and for the losses in the ion current, leading to an increasing signal-to-noise ratio over time.

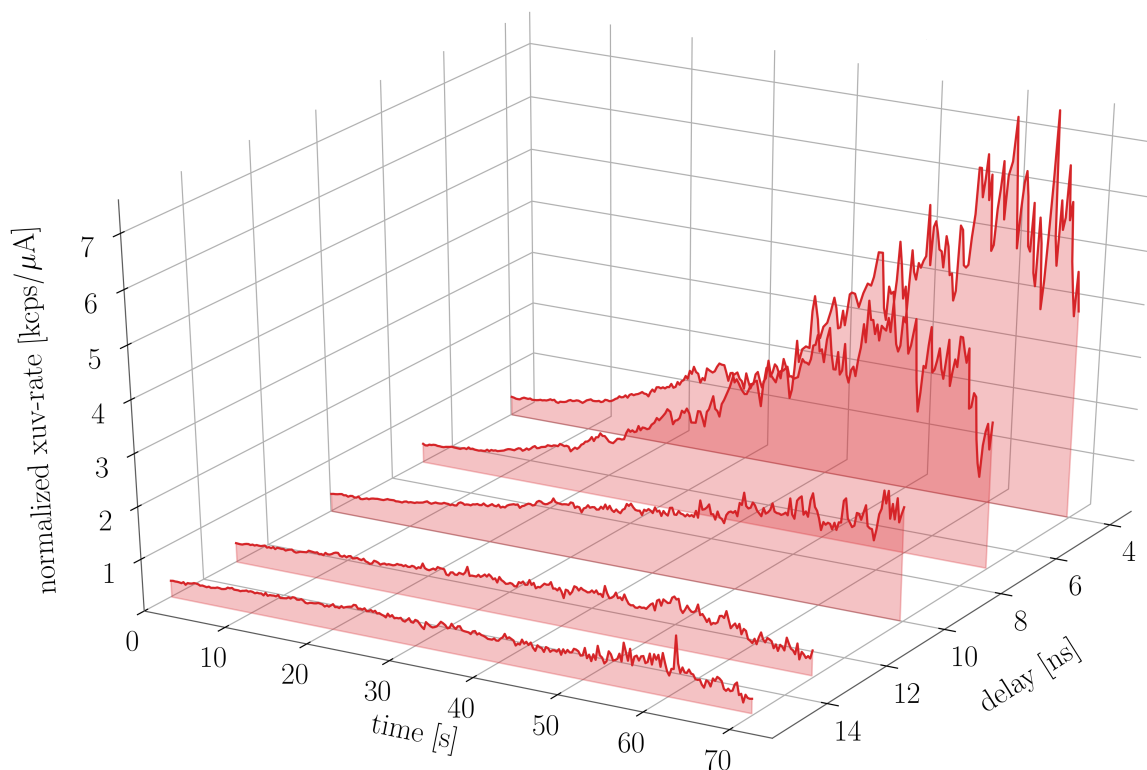


**Figure 3.** Fluorescence rate of  $^{12}\text{C}^{3+}$  ions plotted as a function of the delay of the laser pulses with respect to the ion bunches, as detected by the XUV detection system at the ESR. For these measurements, there were 7 ion bunches stored in the ESR, the repetition rate of the laser pulses was  $\sim 9$  MHz, and the laser wavelength was 257.235 nm.

Depending on the delay of the laser pulses and the consequently shifted overlap region in the straight section of the ESR, the fluorescence rate decreased for longer delays, as depicted in Figure 3. The maximum fluorescence rate was observed at a laser pulse delay of around 4 ns. This can be understood in terms of ion bunches being laser-excited and decaying ( $\sim 4$  ns later) just in front of the XUV detector. It can also clearly be seen that the fluorescence rate practically vanishes when the delay is not properly chosen.

#### 4. Conclusions

The rate of fluorescence photons emitted from the laser-excited ions and measured by the in vacuo XUV detector system serves as a diagnostic tool to determine the transition wavelength in the coasting ion beam mode and to synchronize the laser pulses with the ion bunches in the bunched ion beam mode. The latter scenario is very important for future laser cooling and laser spectroscopy studies at FAIR (SIS100). The improved XUV detector

was successfully redeployed, and more results from the experiment will be published in the near future.

## 5. Outlook

Currently being developed and built is a fluorescence detection and spectroscopy system for the laser cooling project at the upcoming SIS100 synchrotron. The new dispersed fluorescence detection system uses an aberration-corrected laminar grating in grazing incidence geometry which diffracts photons dependent on their wavelengths. An open-face micro-channel plate detector in a Chevron stack configuration (sensitive to the soft X-ray regime) with a position-sensitive delay-line readout ( $\leq 0.5$  ns time resolution) is used for spectrally resolved detection. If no energy resolution is required, the system can also be used for direct detection of the fluorescence photons with a significantly larger acceptance.

**Author Contributions:** P.S., M.S. (Markus Steck) and D.W. conceived and organized the experiment. D.K., S.K., B.L. and T.W. developed the TU Darmstadt pulsed laser system. K.U., V.H., D.W. and C.W. developed the XUV detector. S.K. prepared the data acquisition system. K.U., L.B., M.B., N.E., V.H., M.H., N.K., S.K., T.K., B.L., R.S., M.S. (Mathias Siebold), M.S. (Markus Steck) and D.W. worked on experimental shifts. K.U., S.K. and B.L. performed the analysis of the data. M.B., X.M., W.N., U.S., P.S., T.S., T.W. and C.W. were supervisors and participated in reviewing and editing of the paper together with M.L., H.W., W.W., K.U., B.L., V.H., S.K. and D.W. prepared the manuscript. All authors have read and agreed to the published version of the manuscript.

**Funding:** This work has been supported by the BMBF under contract numbers 05P19PMFA1 and 05P21RDFA1.

**Institutional Review Board Statement:** Not applicable.

**Informed Consent Statement:** Not applicable.

**Data Availability Statement:** Data available on request.

**Conflicts of Interest:** The authors declare no conflict of interest.

## References

1. Franzke, B. The heavy ion storage and cooler ring project ESR at GSI. *Nucl. Instrum. Methods Phys.* **1987**, *24–25*, 18–25. [CrossRef]
2. Steck, M.; Beckert, K.; Beller, P.; Franzke, B.; Nolden, F. Experimental Progress in Fast Cooling in the ESR. In Proceedings of the IEEE Particle Accelerator Conference, Knoxville, TN, USA, 16–20 May 2005; Volume 2005, pp. 615–619. [CrossRef]
3. Winters, D.; Beck, T.; Birkel, G.; Dimopoulou, C.; Hannen, V.; Kühl, T.; Lochmann, M.; Loeser, M.; Ma, X.; Nolden, F.; et al. Laser cooling of relativistic heavy-ion beams for FAIR. *Phys. Scr.* **2015**, *T166*, 014048. [CrossRef]
4. Hangst, J.S.; Nielsen, J.S.; Poulsen, O.; Shi, P.; Schiffer, J.P. Laser Cooling of a Bunched Beam in a Synchrotron Storage Ring. *Phys. Rev. Lett.* **1995**, *74*, 4432–4435. [CrossRef] [PubMed]
5. Atutov, S.N.; Calabrese, R.; Grimm, R.; Guidi, V.; Lauer, I.; Lenisa, P.; Luger, V.; Mariotti, E.; Moi, L.; Peters, A.; et al. “White-light” Laser Cooling of a Fast Stored Ion Beam. *Phys. Rev. Lett.* **1998**, *80*, 2129–2132. [CrossRef]
6. Buß, A. Development of Fluorescence Detectors for Laser Spectroscopy Experiments at GSI/FAIR, and Measurement of Hyperfine Transitions between the  $2^3P$  and  $2^3S$  States in Helium-like Boron. Ph.D. Thesis, University of Münster, Münster, Germany, 2021.
7. Klammer, S. Einsatz Gepulster UV Lasersysteme zur Kühlung Hochrelativistischer Ionenstrahlen und Laserspektroskopie an Beryllium-ähnlichen Krypton-Ionen. Ph.D. Thesis, Technische Universität Darmstadt, Darmstadt, Germany, 2022. [CrossRef]
8. Winzen, D.; Hannen, V.; Busmann, M.; Buß, A.; Egelkamp, C.; Eidam, L.; Huang, Z.; Kiefer, D.; Klammer, S.; Kühl, T.; et al. Laser spectroscopy of the  $2S_{1/2} - 2P_{1/2}, 2P_{3/2}$  transitions in stored and cooled relativistic  $C^{3+}$  ions. *Sci. Rep.* **2021**, *11*, 9370. [CrossRef]
9. Winters, D.F.A.; Kühl, T.; Schneider, D.H.; Indelicato, P.; Reuschl, R.; Schuch, R.; Lindroth, E.; Stöhlker, T. Laser spectroscopy of the  $(1s^2 2s2p) ^3P_0 - ^3P_1$  level splitting in Be-like krypton. *Phys. Scr.* **2011**, *2011*, 014013. [CrossRef]
10. Busmann, M. Laser Cooling of Ion Beams at Relativistic Energies. *ICFA Beam Dyn. Newslett.* **2014**, *65*, 8–21. Available online: [https://icfa-usa.jlab.org/archive/newsletter/icfa\\_bd\\_nl\\_65.pdf](https://icfa-usa.jlab.org/archive/newsletter/icfa_bd_nl_65.pdf) (accessed on 6 February 2023).

**Disclaimer/Publisher’s Note:** The statements, opinions and data contained in all publications are solely those of the individual author(s) and contributor(s) and not of MDPI and/or the editor(s). MDPI and/or the editor(s) disclaim responsibility for any injury to people or property resulting from any ideas, methods, instructions or products referred to in the content.